Quantitative Analysis of Tendon Structural Integrity in Chickens using Fourier Transform-Second Harmonic Generation Imaging

Mayandi Sivaguru[1], James D Richards[2], Julia J Dibner[2], John Paul Eichorst[1,3], Terra D Wineman[2] and Juxing Chen[2*]

[1]Institute for Genomic Biology, University of Illinois Urbana-Champaign, 1206 West Gregory Drive, Urbana, Illinois 61801, USA

[2]Novus International Inc. 20 Research Park Drive, St Charles, Missouri 63304, USA

[3]University of Minnesota – Twin Cities, Medicine – PACCS, 116 Church St SE, Minneapolis 55455, USA

*Corresponding author: Juxing Chen, Novus International Inc. 20 Research Park Drive, St Charles, Missouri 63304, USA, Tel: 636-926-7418; Fax: 636-926-7449; E-mail: juxing.chen@novusint.com

Abstract

Degenerative changes in tendons are common in human and land-dwelling vertebrates of all species, and are associated with both age and use. Tendon rupture and inflammation are common causes of lameness in broilers and breeders at multiple ages and has become a very important issue in the poultry industry attempts to analyze tendon health have relied primarily on visual assessment. The ability to conduct meaningful experiments on causes and interventions would be much improved by a direct assay of tendon structural integrity. The objective of this study is to test whether we can use Fourier transform-second harmonic generation (FT-SHG) imaging technique to quantify the differences in collagen fiber organization and nuclei morphology between normal and injured chicken tendons. Tendon injury/degeneration was induced by rearing chickens in wire-floor pens and feeding them an oxidized fat diet. Injured tendons had greater collagen fiber degradation/degeneration; more randomly organized collagen fibers, higher cellularity and more circular-shaped nuclei than normal tendons, indicating loss of collagen tertiary structure and lateral compression in injured tendons. Therefore, analysis of collagen fiber organization and nuclear morphology using FT-SHG imaging is a potential diagnostic tool to evaluate tendon structural health and to test the effects of nutrients and intervention strategies on the structural development of tendons in chickens.

Keywords: Tendon; Collagen fiber; Nuclei morphology; Fourier Transform-Second Harmonic Generation; Chicken

Introduction

Collagen fibers are the main structural component of tendons. Degenerative changes in tendons are common in land-dwelling vertebrates of all species, and are associated with both age and use. Attempts to analyze tendon health have relied primarily on visual assessment. Morphological changes in the collagen fiber's organization are associated with tendon pathology [1-3]. Various techniques have been developed to assess collagen structural health. For example, researchers have used quantitative polarized-light microscopy to detect the degree of collagen parallelism in cartilage of porcine joints [4] and to evaluate collagen fiber organization in horse tendons [5]. Second harmonic generation using two-photon microscopy is the most recent modality in microscopy for analyzing collagen organization due to the strong non-centro-symmetric nature of the collagen's molecular arrangement in nature [6,7]. Recently, we have developed a quantitative SHG imaging and analysis technique using Fast Fourier Transformation (FT-SHG) [8] to quantify and analyze collagen fiber organization in horse tendons [5,9]. Similar investigation was performed at different levels in a multitude of organisms where collagen plays a pivotal role in maintaining the integrity of tissue structure such as rat tail tendon [10] and porcine tendon [11]. Automated SHG imaging analysis has been developed to quantify the amount of matrix disorganization in rat patellar [12], rat tail tendons, mouse skin, bovine corneas, and human corneas [10]. FT-SHG can quantify the extent of collagen disorganization in different tissue types in multiple species and is therefore proving to be a much more powerful tool than other methods, such as polarized light microscopy, to evaluate tendon health and collagen quality [5].

Tendon degeneration is the most common histological finding in spontaneous tendon ruptures, and it may result in lower tensile strength and a predisposition to rupture [13]. Rupture of the gastrocnemius tendon is a recognized cause of lameness in broilers and breeders at multiple ages and has become a very important issue in the poultry industry [14-17]. Lameness is the fourth leading cause of economic loss in the U.S. poultry industry, according to a recent survey of U.S. broiler veterinarians. As of 2000, lameness issues cost the poultry industry in the U.S. more than $120 million per year [18], and undoubtedly, this number has increased. To our knowledge, there is no published method to address tendon damage and quantitatively analyze and relate collagen fiber organization in chickens to tendon damage. Given that tendon rupture is a common cause of lameness and economic loss in poultry production, it would be useful to establish a method to assess tendon structure differences between normal tendon and damaged tendons. Biochemical force plays an important role in tendon rupture [15,16]. Mechanical stress leads to the accumulation of damaging free radicals and oxidative stress in articular cartilage tissues [19]. Oxidative stress has been reported to exacerbate joint disease in a rat arthritis model [20] and associate with cartilage degeneration in an experimental canine model of osteoarthritis [21]. Dietary oxidized oil has been reported to induce oxidative stress in animals [22].

In this study, broiler chickens were reared in pens with wire ramps to impose mechanical stress for their leg joints [23] and were fed an oxidized fat diet to induce oxidative stress. A normal fat diet was used as a control. The combination of mechanical stress and diet-induced

oxidative stress resulted in severe hock lesions and tendon injury and higher incidence of lameness in broiler chickens. The purpose of this study is to determine whether FT-SHG imaging can be used as a technique to quantify the structural differences between normal tendon and injured/degenerated tendon. To maximize the possibility to detect differences between control and injured tendons, control gastrocnemius tendons were dissected from two non-lame birds fed the normal diet; injured gastrocnemius tendons were dissected from two lame birds fed the oxidized fat diet. We analyzed the differences of collagen organization and nuclei morphology between control tendons and injured tendons by calculating the abundances of spatial frequencies present with Fourier-based techniques.

Materials and Methods

Reagents

Notox was purchased from Scientific Device Laboratory (Des Plaines, IL, USA). Vitamin E was purchased from Teklad Lab Animal Diets - Harlan. OCT and ultra-pure sucrose were purchased from Tissue Tek (Sakura Fine Tek) and Plant media, respectively.

Bird trials and tissue sample preparation

Animal protocols at Novus International, Inc. are conducted in accordance with established Standard Operating Procedures (SOPs). All SOPs are departmentally reviewed and subsequently approved by the originator, Senior Manager, Animal Testing and Facilities, and the Director of Animal Nutrition Research. Additionally, animal facilities are reviewed monthly by an external veterinarian for animal health, animal care, and facility cleanliness and suitability for animal research. Protocols or SOPs involving invasive procedures are reviewed and carried out by licensed veterinarians. By law, Novus International, Inc. is not required to maintain an Animal Care and Use Committee. However, the procedures followed to isolate the tendons for the current trial are the same as in our previous work with horse tendons [5] which was approved by the University of Illinois Animal Care and Use Committee.

In this study, male broiler chickens were reared in 5 ft ×10 ft wire flooring pens with wood shaving litter on top of the wire. Chicken's feed was put on one side and water was put on the opposite side (Figures 1A and B). In the first three weeks, the wire floor was kept flat for young broilers to grow. On day 22, a ramp was raised about 45 degrees, which forced the birds to walk up the ramp to drink and walk down the ramp to eat (Figures 1A and B). This causes mechanical stress in their legs, including their tendons. Birds were fed a common commercial-type diet until day 8. Oxidized oil induced oxidative stress in animals [22], which can then cause tendon damage [20]. To exacerbate the stress to tendon, birds in one pen (Figure 1B) were fed oxidized fat diet that included 5% oxidized soybean oil starting on day 8. As a control, birds in the other pen (Figure 1A) were then fed a normal fat diet that included 5% stabilized (non-oxidized) soybean oil. Soybean oil was oxidized by continuously bubbling air and heating to 100°C (Over-limit temperature is 105°C) at a rate of 3 CFM using JKEM HCC-230 Temperature Controller and Drum Heaters. Peroxide values were determined every few hours until the peroxide value of the oil was approximately 225 meq/kg (11.25 mEq/kg in the diet).

On day 55, 1 cm sections from the distal end of osteotendineal junction were cut and fixed in Notox (Scientific Device Laboratory, Des Plaines, IL) for one hour, followed by washing three times with PBS (phosphate buffered saline), incubated with PBS/10% sucrose for two hours, PBS/20% sucrose for two hours, and then PBS/30% sucrose overnight. The tendons were then embedded in cryostat mold using 50% OCT/50% PBS containing 30% sucrose.

Sectioning and labeling nuclei

For cryostat sectioning, the samples were brought to -20°C from -80°C storage temperature and cut to 20 µm-thick sections [optimized for SHG microscopy as described previously [5,9] using a cryostat (Leica CM3050S). The sections were then thawed, secured between two cover glasses (#1.5) with or without the nuclear counter stain Propidium Iodide (PI-emission wavelength over 565 nm) from Life Technologies (Eugene, OR) and imaged fresh or within 24 hours. For each tendon sample, 4-6 2D images of specific locations (distal part of the tendon) were taken. For the morphometric analysis, 2D images of nuclei from each image of a given replicate are pooled by superimposing all available images.

Second harmonic generation microscopy of collagen - experimental set up

The experimental setup used for SHG microscopy was a modified Zeiss LSM 710 system described previously [9], which is equipped with a tunable Ti: Sapphire laser source that produces 70 fs pulses at a repetition rate of 80 MHz. The excitation wavelength used in this study was 780 nm and a quarter wave plate was placed in the path of the excitation laser used to generate circularly polarized light (the fundamental laser is plane polarized) for gathering isotropic SHG signal from collagen fibers at all orientations in a single image [9]. The LSM 710 scanner was used to scan the beam in a raster pattern. The exciting beam was reflected by a short-pass 760 nm dichroic beam splitter (everything above 760 nm is reflected and below transmitted) and focused onto the sample using a 40x C Apochromat 1.2 NA water-immersion objective. The emitted backward SHG signal was collected by the same objective, while the forward signal was collected by a 0.55 NA objective. Two filters were positioned in each geometric image acquisition (forward and backward): one filter (Semrock FF01-680/SP-25) was used to block the laser wavelengths, and the other (Semrock FF01-390/18-25) was a band-pass filter to transmit the SHG signal (390 nm). Photomultiplier tubes (Hamamatsu R6357 multi-alkali) recorded the forward and backward SHG images.

Two-Photon Fluorescence Microscopy of Nuclei

While collecting SHG, simultaneously the images for PI-labeled nuclei fluorescence (two photon fluorescence microscopy - TPFM) were taken using additional detectors in the path of non-descanned detection (NDD detectors) with corresponding emission filters using the same excitation for SHG (780 nm). A 565 nm-long pass emission filter was used after the backward SHG detection path using a 400 LP dichroic mirror. The average power was 3 mW. Parameters such as detector gain, pixel dwell time, and frame averaging were maintained constantly when acquiring images in the forward and backward directions.
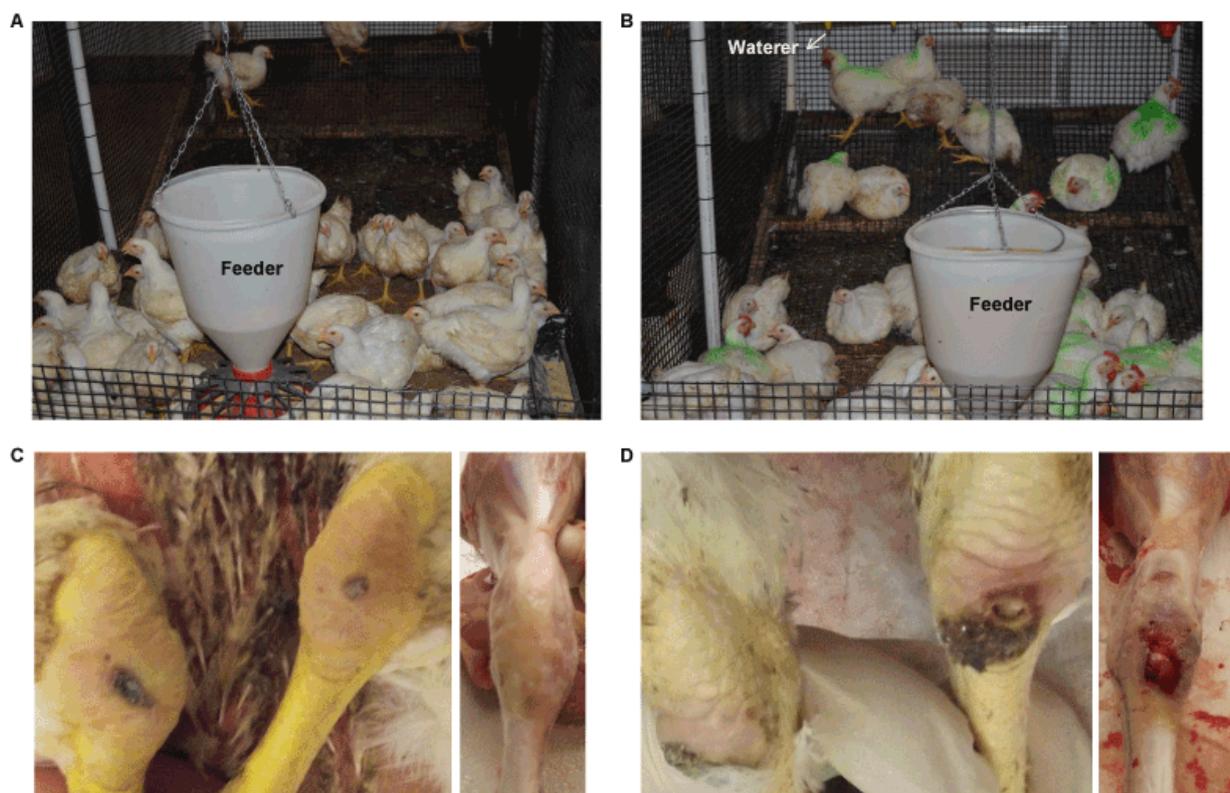
Figure 1: Broiler chicken in pens with ramp and their hock lesions. A. Chicken fed a normal fat diet in pen with ramp. B. Chicken fed an oxidized fat diet in pen with ramp. C, Hock lesion of chicken fed a normal fat diet. D. Hock lesion of chicken fed an oxidized fat diet.

Fourier transformation analysis of collagen

A modified FT-SHG code was used to assess collagen fiber organization and intensity based on the distribution of spatial frequencies present in an image [5]. This code is available for download at the FTP site maintained by the Core Facilities at the University of Illinois at Urbana-Champaign. Please contact the corresponding author to receive instructions for downloading. As described previously, the orientation of distribution of spatial frequencies dictates the orientation of the underlying structures. For example, in Figure 2A, a grating of varying intensity was simulated and rotated. As a result of the rotation, the distribution of spatial frequencies depicted in Figure 2B rotates in equal increments of angle. In this example, the histogram of spatial frequencies contains an axis parallel and an axis perpendicular to the lines in the grating. Therefore, even visually, the orientation of the grating can be determined simply by looking at the histogram of spatial frequencies. In biological samples such as collagen, this technique is extremely sensitive to changes in orientation throughout an image. In Figure 2C, the fibers of collagen are aligned in two distinct orientations. As a result, the distribution of spatial frequencies (Figure 2D), contains distinct lobes corresponding to the two orientations of collagen in the image.

Fourier transformation analysis of nuclei morphology

The morphometric analysis of nuclei was performed in the Axiovision (Carl Zeiss, Jena, Germany) program using standard parameters, such as area, perimeter, counts, and ellipse major and minor, on individual images. All available replicate nuclear images were overlaid and the FFT was performed and the outline of the FFT shape is obtained in the program Image J [24]. The FFT outlines were calculated after the images are thresholded (the thresholded raw data is provided in Figure 3), to pick up the central distribution of frequencies against the dark background, converted to binary, applied fill holes binary function, outliers are removed using a 10 pixel radius using the Remove Dark Outlier module, then finally the binary image is applied with an outline tool, which renders the outline in the same program Image J. This image is saved in RGB format and to distinguish the three replicates, they were psuedocolored using the curve function in the Adobe Photoshop (Adobe Systems, San Jose, CA) leaving one color per image and by removing other two channels in RGB. Finally, in the same program, all three outlines are superimposed in a single image with the black background using the screen function as to visualize all three outlines in one image.
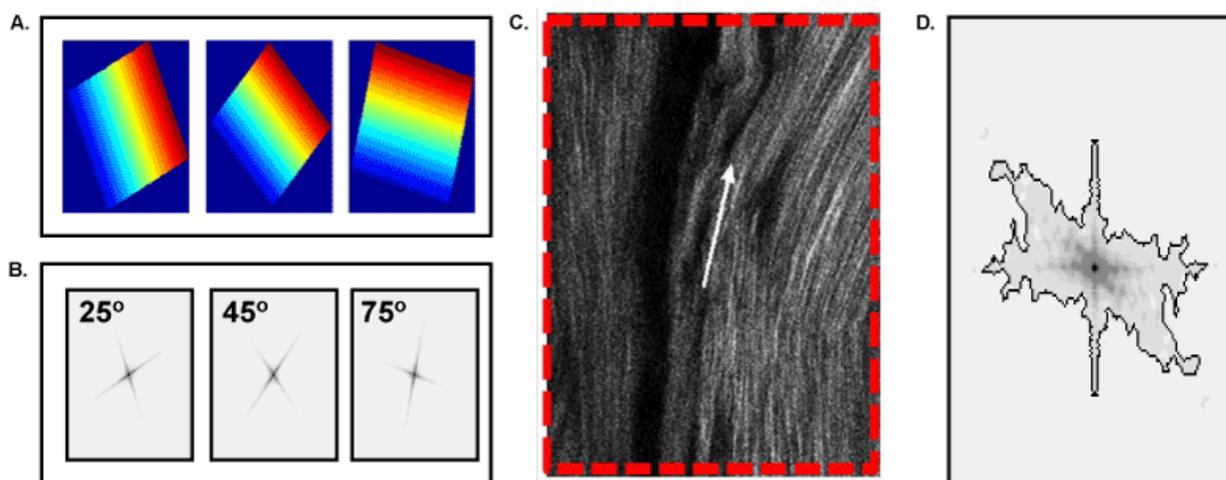
Figure 2: Fourier-based calculation of orientation: (A) A grating of varying intensity was simulated and rotated through a set of 3 angles (25°, 45° and 75°). (B) The histogram of spatial frequencies corresponding to each image in (A) is presented. (C) An image of collagen fibers is presented containing two distinct orientations of the fibers. The white arrow indicates the average orientation of the fibers. (D) The histogram of spatial frequencies derived from (C) clearly contains two lobes indicative of the two distinct orientations of collagen.

Data statistical analysis

The variance of nuclei and collagen organization data was analyzed using the General Linear Models procedure of SAS (SAS institute, 1992). Individual tendon was used as experimental unit in this study.

Results

### Oxidative stress and ramp induced lameness and tendon injury in broiler chicken

On day 55, birds fed an oxidized fat diet had more severe hock lesion and higher incidence of lameness (16.7%) compared to birds fed normal diet (7.5%) (Figures 1C and D). The purpose of this study is to determine whether FT-SHG imaging can be used to quantify the structural differences between normal tendon and injured/damaged tendon. Therefore, on day 55, the normal tendons (Control) were collected from two non-lame birds fed the normal diet; the "worst" tendons (Injured) were collected from two lame birds fed the oxidized fat diet. This gave us the best opportunity to see the structural differences between control and Injured tendons. Most FT-SHG images from control tendons exhibited regular crimping and parallel alignment of collagen fibers along the axis of the load (Figure 4A). Most FT-SHG images of injured tendons had disorganized crimping and a non-parallel layout of collagen fibers lacking tight connections between collagen fibers (Figure 4B).

Injured tendons had more disorganized collagen fibers than control tendons

Collagen fiber organization in tendon was assessed using a modified FT-SHG code as described above. In this analysis, 4-6 images were taken from each tendon and each image was divided into 64 tiles. Each tile is 26.6 µm by 26.6 µm. The tiles containing insufficient intensities to calculate the orientation of the collagen (less than 275 counts) were defined as dark regions (blue highlighted tiles), which indicates collagen degradation and weak/loss of collagen fiber. The tiles with no preferred collagen fiber orientation (randomly organized fibers) were defined as isotropic regions (pink highlighted tiles). In other words, when the distribution of spatial frequencies was estimated as an ellipse, any tile in which the length of the major axis divided by the length of the minor axis was less than 1.3 was considered isotropic.

The corresponding FFT images in injured tendons (Figure 5 lower panel) have a broader frequency distribution (oval to circular) when compared to control tendons (Figure 6 lower panel). The collagen fibers in injure tendons look more randomly and irregularly organized (Figure 5 upper panel) compared to control tendons (Figure 6 upper panel). Quantitative data showed that the percentage of isotropic regions, dark regions, and total disorganized regions (dark region + isotropic region) increased by 3.7 fold (p=0.0178), 2.6 fold (p=0.1145), and 3.2 fold (p=0.0113), respectively, in injured tendons when compared to control tendons (Figure 7). These results clearly indicating that collagen fibers in injured tendons were much more disorganized than control tendons.
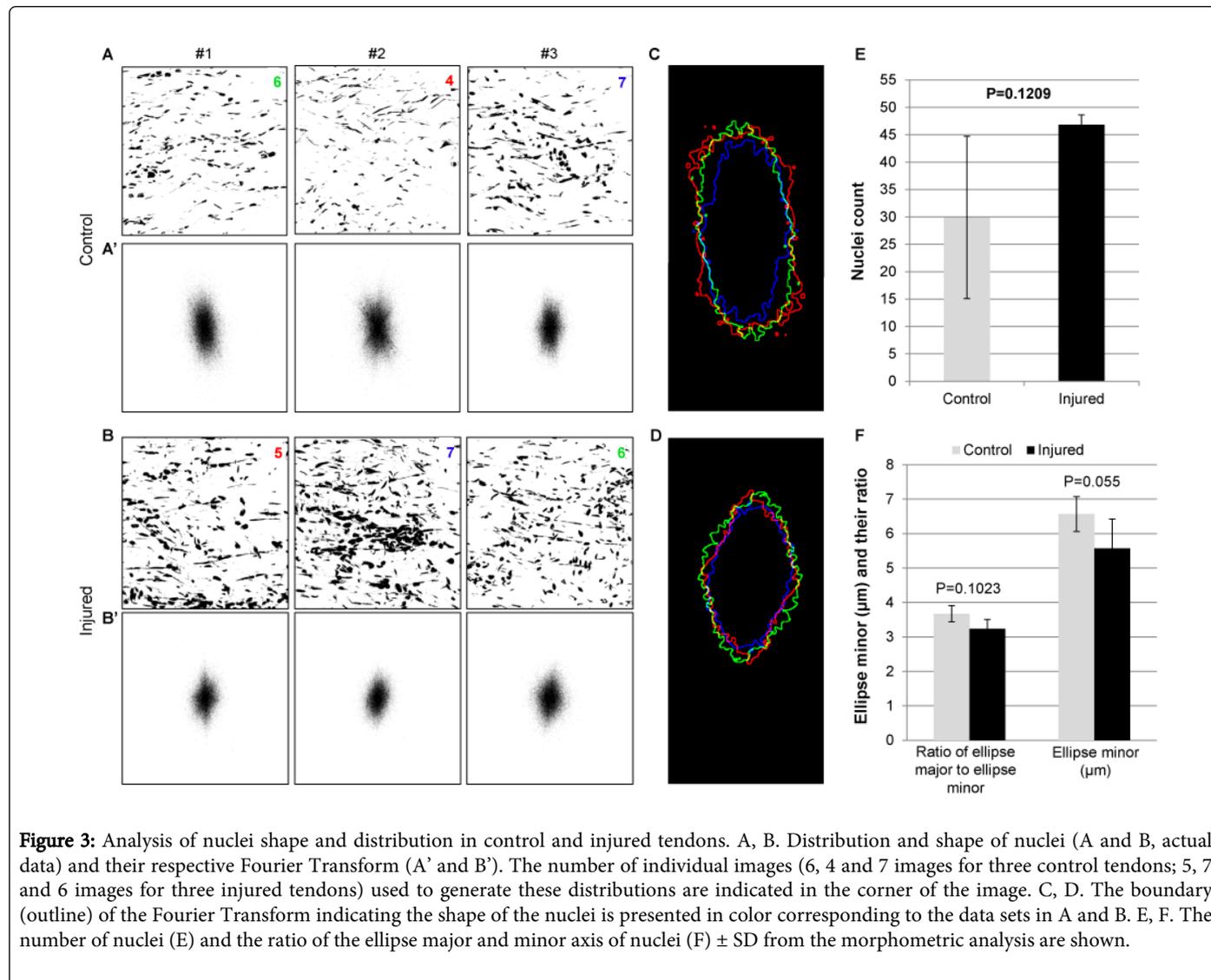
Figure 3: Analysis of nuclei shape and distribution in control and injured tendons. A, B. Distribution and shape of nuclei (A and B, actual data) and their respective Fourier Transform (A' and B'). The number of individual images (6, 4 and 7 images for three control tendons; 5, 7 and 6 images for three injured tendons) used to generate these distributions are indicated in the corner of the image. C, D. The boundary (outline) of the Fourier Transform indicating the shape of the nuclei is presented in color corresponding to the data sets in A and B. E, F. The number of nuclei (E) and the ratio of the ellipse major and minor axis of nuclei (F) ± SD from the morphometric analysis are shown.

Injured tendons had increased cellularity and circular nuclei than that of control tendons

The number and characteristic of nuclei was measured by Fourier analysis to understand the cellularity (increased or decreased number of cells), as well as the distribution and morphology (shape) of cells contained in the control and injured tendons. The distribution (shape and density) of nuclei in three control tendons was similar (Figure 3A). Likewise, the distribution (shape and density) of nuclei in injured tendons was also similar (Figure 3B). However, clear difference in the shape and density of nuclei were observed between control and injured tendons (Figure 3A, B). To be more quantitative, the shape of nuclei from FFT analysis was elliptical-shape in control tendons (Figure 3C),

indicating the presence of lateral compression, circular- and diamond-shape in injured tendons (Figure 3D), suggesting the loss of lateral compression due to collagen damage and degeneration. Further, the number of nuclei in injured tendons numerically increased by 1.56 fold compared to that of control tendons (p=0.1209) (Figure 3E). The ratio of ellipse major to ellipse minor, an indicator of nuclei's roundness or circularity, numerically decreased by 12% in injured tendons compared to control tendons (p=0.1023), which is mainly due to the 15% decrease of ellipse minor (p=0.055) (Figure 3F). These results suggest that the nuclei from injured tendons have a tendency of not towing the same morphology and distribution compared to their control counterparts.
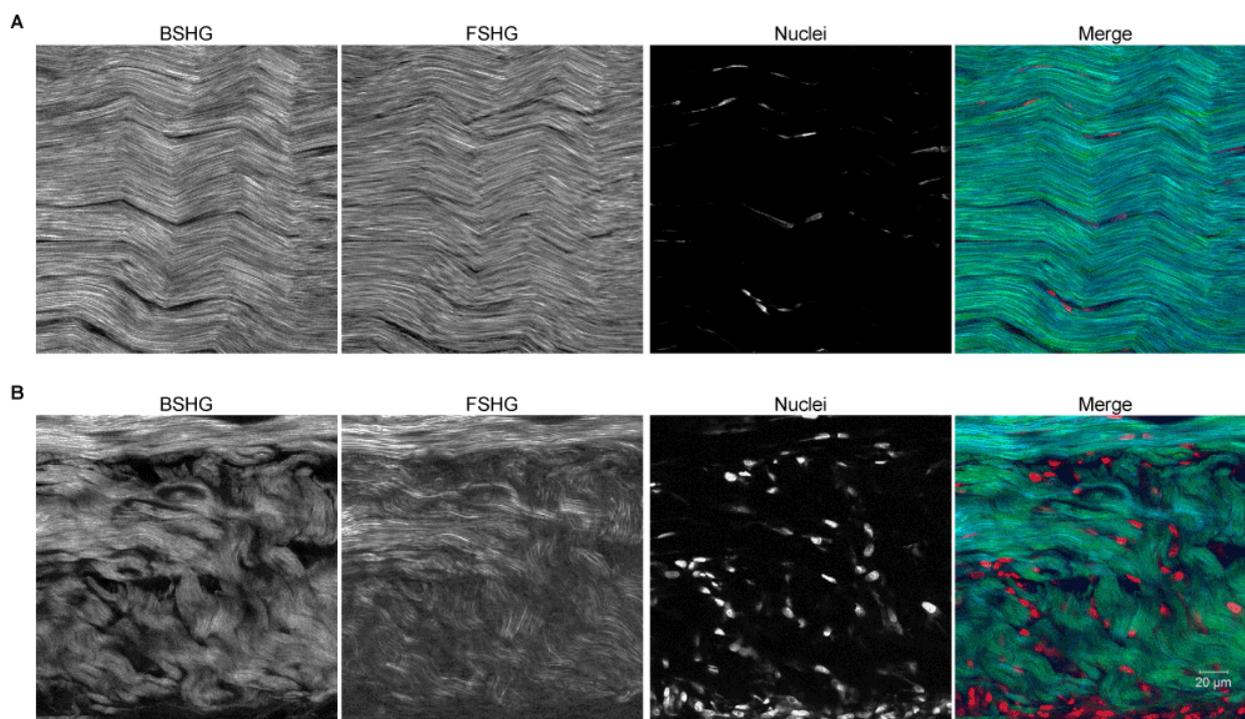
Figure 4: SHG images of control and injured gastrocnemius tendons on day 55. Control tendons were collected from non-lame birds fed normal fat diet. Injured tendons were collected from lame birds fed oxidized fat diet. Collagen fibers were imaged with both forward SHG (blue in merge images) and backward SHG (green in merge images) modalities while nuclei were imaged with TPFM (two-photon fluorescence microscopy) counter-stained with PI (red). The individual channels (BSHG, FSHG and TPFM) are shown in grey scale for clarity. Scale bar indicates 20 μm.

Discussion

The matrix of collagen in the tendon constantly remodels itself, especially with higher rates of turnover at the sites exposed to excess strain or mechanical stress [25]. In response to stress such as micro trauma, repetitive overload and oxidative stress, tendons have to undergo active repair of degeneration by either degeneration of tendon itself, inflammation of the tendon sheath or a combination of both, otherwise the tendon would weaken and rupture eventually [26,27]. Tendon repair and regeneration includes three stages: tissue inflammation, cell proliferation and remodeling [28]. Inflammation can provoke the release of growth factors and cytokines [29], which then stimulate tenocyte proliferation and collagen synthesis and improve tendon healing [30].

Collagen fibers in normal tendons develop and grow in parallel and are bundled tightly with a wavy configuration (also called crimping), which facilitates a 1-3% elongation of the tendon [31]. However, collagen fibers in tendinopathic samples are loose, unequally and irregularly crimped with increased waviness [32-36], which is an indication of the loss of lateral tension or tertiary structure [9]. Rat patellar tendons loaded with moderate-level fatigue had widened inter-fiber space [37,38]. Therefore, disorganized collagen fiber with increased waviness and inter-fiber space is a sign of tendon degeneration and repair.

Tenoblasts and tenocytes form up to 95% of cellular contents of the tendon. Tenoblasts are precursor cells of tenocytes and can ultimately differentiate into tenocytes to resolve tendon healing [39]. Tenocytes are terminally differentiated cells with limited proliferation ability. As mature cells, tenocytes have elongated and flattened nuclei which often distribute evenly between collagen fibers; in contrast, tenoblasts are relatively round cells with large ovoid nuclei which initiate tendon repair process through proliferation and migration and often form a cluster with a localized pericellular region devoid of collagen fibers [39]. In tendinopathic tendons, tendon cells are abnormally high in numbers in some areas and have round nuclei [40-42]. Therefore, increase of cellularity and nuclear roundness are also the signs of tendon degeneration and associated repair [43].
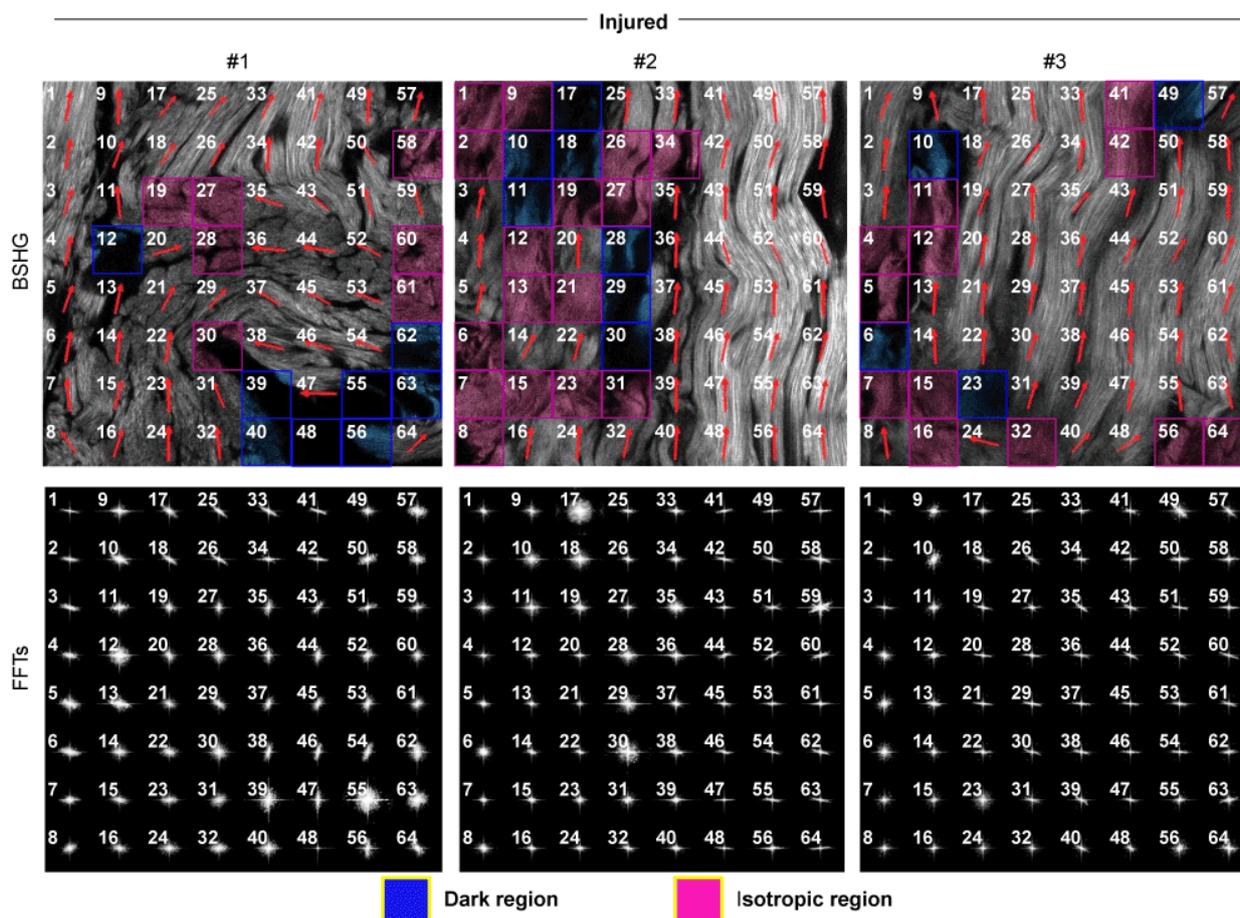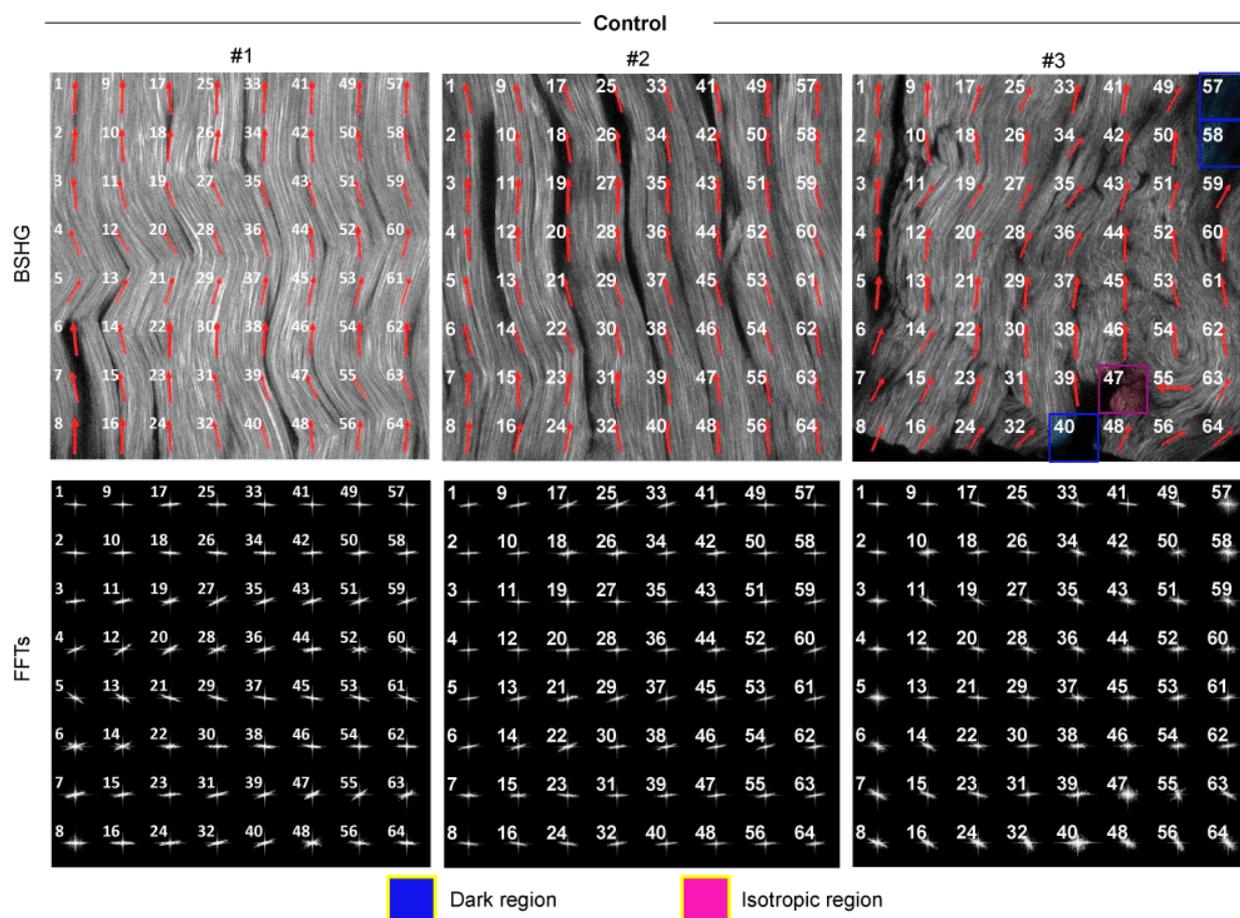
Figure 5: FT-SHG imaging and analysis of collagen fiber organization in injured tendons. Preferred orientation angles (indicated by arrows) of collagen fibers were determined using BSHG images. Each image was divided into an 8x8 tile and each tile (a total of 64) was analyzed independently to determine the angle (A, B and C). The 2D Fourier transform of the same tiles was shown in D, E and F. Isotropic regions (tiles) where the collagen fiber orientation cannot be determined are highlighted in pink. Dark regions (tiles) where there was not enough measured signal (below threshold) to calculate an orientation of the fibers are highlighted in blue.

In this study, injured tendons had increased levels of randomly organized collagen fibers (isotropic regions) and weak signals suggesting the loss of definable collagen fibers from the SHG generated by the collagen (dark region) than control tendons. We found that the injured tendons tended to have more and circular nuclei. The round nuclei were accumulated in the area where collagen fibers were disorganized, and they might be belonged to either tenoblasts or inflammatory cells. This indicates that tissue inflammation and/or cell proliferation may happen at the same time to repair the damaged tendon. The increase of cellularity and accumulation of tenoblasts suggest that tenoblasts proliferate and migrate into a wounded region to synthesize collagen and initiate tendon repair process, indicating a high demand of new collagen synthesis to repair tendon damage. The nature of these cells and their healing ability though is beyond the scope of this present study but efforts will be made in the future to investigate this topic.

Oxidized fat diet increased the severity of hock lesions and incidence of lameness, so we hypothesize that both lameness and tendon degeneration/injury are primarily caused by oxidative stress. Future studies will determine whether the tendon injury is caused by oxidative stress, lameness or both using a two-factorial design, and test whether dietary anti-oxidants can be used as an intervention strategy to attenuate tendon injury/rupture and to reduce the incidence of associated lameness in poultry industry.

Figure 6: FT-SHG imaging and analysis of collagen fiber organization in control tendons. Data were analyzed as described in Figure 4.

To conclude, here we described the first absolute and quantitative assessment of collagen organization in the tendons of broiler chickens and found clear differences between normal and injured or damaged tendons. The modified FT-SHG technique translates specifically and detects the absolute extent of both collagen fiber organization and damage. The tiled metrics derived from this analysis while provide precise location of the damage across the image it can also eliminate the subjectivity in diagnosis. Finally, because the Fast Fourier Transform is an extremely rapid calculation and make the real-time analysis of tendon injury a possibility which renders this technique as a potential diagnostic tool in clinical setting to evaluate tendon structural health and intervention strategies in any vertebrate animals.

Acknowledgements
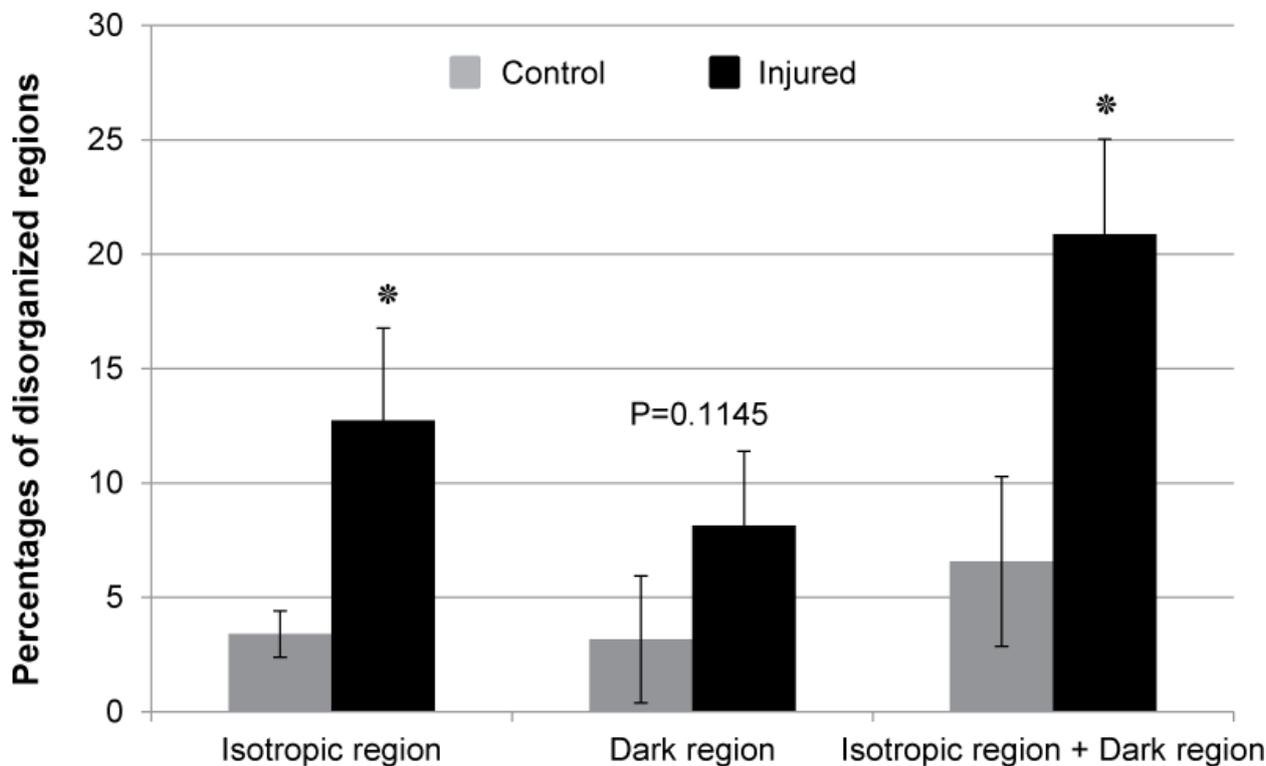
Figure 7: The percentages ± SD of isotropic regions and dark regions in control and injured tendons. ˙indicates significant differences between control and injured tendons.

Funding

References

1. Kannus P, Józsa L (1991) Histopathological changes preceding spontaneous rupture of a tendon. A controlled study of 891 patients. J Bone Joint Surg Am 73: 1507-1525.

2. Kastelic J, Baer E (1980) Deformation in tendon collagen. Symp Soc Exp Biol 34: 397-435.

3. Sonnabend DH, Yu Y, Howlett CR, Harper GD, Walsh WR (2001) Laminated tears of the human rotator cuff: a histologic and immunochemical study. J Shoulder Elbow Surg 10: 109-115.

4. Långsjö TK, Vasara AI, Hyttinen MM, Lammi MJ, Kaukinen A, et al. (2010) Quantitative analysis of collagen network structure and fibril dimensions in cartilage repair with autologous chondrocyte transplantation. Cells Tissues Organs 192: 351-360.

5. Sivaguru M, Durgam S, Ambekar R, Luedtke D, Fried G, et al. (2010) Quantitative analysis of collagen fiber organization in injured tendons using Fourier transform-second harmonic generation imaging. Opt Express 18: 24983-24993.

6. Williams RM, Zipfel WR, Webb WW (2005) Interpreting second-harmonic generation images of collagen I fibrils. Biophys J 88: 1377-1386.

7. Roth S, Freund I (1979) Second harmonic-generation in collagen. J Chem Phys 70: 1637-1643.

8. Brigham EO (1988) The Fast Fourier Transform and Its Application. Prentice Hall, Englewood Cliffs, New Jersey.

9. Sivaguru M, Eichorst JP2, Durgam S3, Fried GA2, Stewart AA3, et al. (2014) Imaging horse tendons using multimodal 2-photon microscopy. Methods 66: 256-267.

10. Ghazaryan A, Tsai HF, Hayrapetyan G, Chen WL, Chen YF, et al. (2013) Analysis of collagen fiber domain organization by Fourier second harmonic generation microscopy. J Biomed Opt 18: 31105.

11. Lau TY, Ambekar R, Toussaint KC (2012) Quantification of collagen fiber organization using three-dimensional Fourier transform-second-harmonic generation imaging. Opt Express 20: 21821-21832.

12. Sereysky JB, Andarawis-Puri N, Ros SJ, Jepsen KJ, Flatow EL (2010) Automated image analysis method for quantifying damage accumulation in tendon. J Biomech 43: 2641-2644.

13. Sharma P, Maffulli N (2006) Biology of tendon injury: healing, modeling and remodeling. J Musculoskelet Neuronal Interact 6: 181-190.

14. Dinev I (2008) Clinical and morphological studies on spontaneous rupture of the gastrocnemius tendon in broiler breeders. Br Poult Sci 49: 7-11.

15. Bradshaw RH, Kirkden RD, Broom DM (2002) A Review of the Aetiology and Pathology of Leg Weakness in Broilers in Relation to Welfare. Avian and Poultry Biology Reviews 13: 45-103.

16. Duff SR, Randall CJ (1986) Tendon lesions in broiler fowls. Res Vet Sci 40: 333-338.

17. Fung DT, Wang VM, Laudier DM, Shine JH, Basta-Pljakic J, et al. (2009) Subrupture tendon fatigue damage. J Orthop Res 27: 264-273.

18. Cook ME (2000) Skeletal deformities and their causes: introduction. Poult Sci 79: 982-984.

19. Milam SB, Zardeneta G, Schmitz JP (1998) Oxidative stress and degenerative temporomandibular joint disease: a proposed hypothesis. J Oral Maxillofac Surg 56: 214-223.

20. Kawai Y, Kubota E, Okabe E (2000) Reactive oxygen species participation in experimentally induced arthritis of the temporomandibular joint in rats. J Dent Res 79: 1489-1495.

21. Goranov NV (2007) Serum markers of lipid peroxidation, antioxidant enzymatic defense, and collagen degradation in an experimental (Pond-Nuki) canine model of osteoarthritis. Vet Clin Pathol 36: 192-195.

22. Boler DD, Fernández-Dueñas DM, Kutzler LW, Zhao J, Harrell RJ, et al. (2012) Effects of oxidized corn oil and a synthetic antioxidant blend on performance, oxidative status of tissues, and fresh meat quality in finishing barrows. J Anim Sci 90: 5159-5169.

23. Wideman RF Jr, Hamal KR, Stark JM, Blankenship J, Lester H, et al. (2012) A wire-flooring model for inducing lameness in broilers: evaluation of probiotics as a prophylactic treatment. Poult Sci 91: 870-883.

24. Schneider CA, Rasband WS, Eliceiri KW (2012) NIH Image to ImageJ: 25 years of image analysis. Nat Methods 9: 671-675.

25. Longo UG, Ronga M, Maffulli N (2009) Achilles tendinopathy. Sports Med Arthrosc 17: 112-126.

26. Ker RF (2002) The implications of the adaptable fatigue quality of tendons for their construction, repair and function. Comp Biochem Physiol A Mol Integr Physiol 133: 987-1000.

27. Birch HL, Wilson AM, Goodship AE (1997) The effect of exercise-induced localised hyperthermia on tendon cell survival. J Exp Biol 200: 1703-1708.

28. James R, Kesturu G, Balian G, Chhabra AB (2008) Tendon: biology, biomechanics, repair, growth factors, and evolving treatment options. J Hand Surg Am 33: 102-112.

29. Evans CH (1999) Cytokines and the role they play in the healing of ligaments and tendons. Sports Med 28: 71-76.

30. Molloy T, Wang Y, Murrell G (2003) The roles of growth factors in tendon and ligament healing. Sports Med 33: 381-394.

31. Khan KM, Cook JL, Bonar F, Harcourt P, Astrom M (1999) Histopathology of common tendinopathies. Update and implications for clinical management. Sports Med 27: 393-408.

32. Järvinen M, Józsa L, Kannus P, Järvinen TL, Kvist M, et al. (1997) Histopathological findings in chronic tendon disorders. Scand J Med Sci Sports 7: 86-95.

33. Waterston SW, Maffulli N, Ewen SW (1997) Subcutaneous rupture of the Achilles tendon: basic science and some aspects of clinical practice. Br J Sports Med 31: 285-298.

34. Hamilton B, Remedios D, Loosemore M, Maffulli N (2008) Achilles tendon rupture in an elite athlete following multiple injection therapies. J Sci Med Sport 11: 566-568.

35. Maffulli N, Kader D (2002) Tendinopathy of tendo achillis. J Bone Joint Surg Br 84: 1-8.

36. Maffulli N, Kenward MG, Testa V, Capasso G, Regine R, et al. (2003) Clinical diagnosis of Achilles tendinopathy with tendinosis. Clin J Sport Med 13: 11-15.

37. Fung DT, Wang VM, Andarawis-Puri N, Basta-Pljakic J, Li Y, et al. (2010) Early response to tendon fatigue damage accumulation in a novel in vivo model. J Biomech 43: 274-279.

38. Neviaser A, Andarawis-Puri N, Flatow E (2012) Basic mechanisms of tendon fatigue damage. J Shoulder Elbow Surg 21: 158-163.

39. Chuen FS, Chuk CY, Ping WY, Nar WW, Kim HL, et al. (2004) Immunohistochemical characterization of cells in adult human patellar tendons. J Histochem Cytochem 52: 1151-1157.

40. Maffulli N, Testa V, Capasso G, Oliva F, Panni AS, et al. (2008) Surgery for chronic Achilles tendinopathy produces worse results in women. Disabil Rehabil 30: 1714-1720.

41. Sharma P, Maffulli N (2005) Tendon injury and tendinopathy: healing and repair. J Bone Joint Surg Am 87: 187-202.

42. Magra M, Maffulli N (2008) Genetic aspects of tendinopathy. J Sci Med Sport 11: 243-247.

43. Murphy PG, Loitz BJ, Frank CB, Hart DA (1994) Influence of exogenous growth factors on the synthesis and secretion of collagen types I and III by explants of normal and healing rabbit ligaments. Biochem Cell Biol 72: 403-409.